

Supplemental Figures and Tables

Epigenetic alteration contributes to the transcriptional reprogramming in T-cell prolymphocytic leukemia

Shulan Tian¹, Henan Zhang², Pan Zhang³⁺, Michael Kalmbach³, Jeong-Heon Lee⁴, Tamas Ordog⁵, Paul J. Hampel⁶, Timothy G. Call⁶, Thomas E. Witzig⁶, Neil E. Kay⁶, Eric W. Klee¹, Susan L. Slager¹, Huihuang Yan¹ & Wei Ding⁶

¹Division of Biomedical Statistics and Informatics, Department of Health Sciences Research, Mayo Clinic, Rochester, MN, USA

²Department of Urology, Mayo Clinic, Rochester, MN, USA

³Division of Information Management and Analytics, Department of Information Technology, Mayo Clinic, Rochester, MN, USA

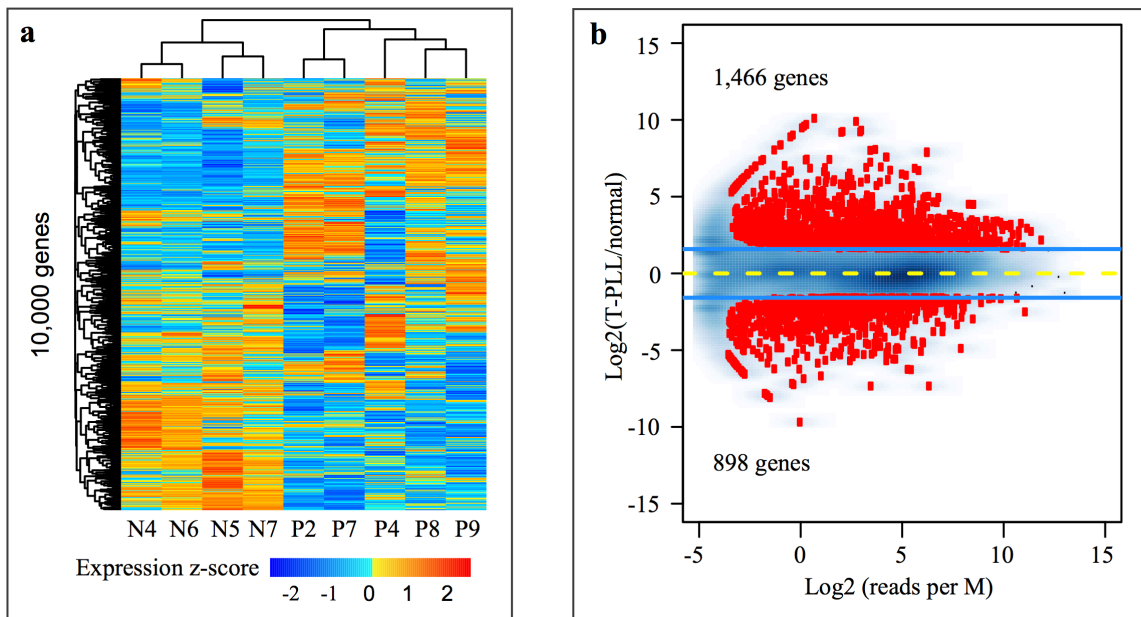
⁴Division of Experimental Pathology and Laboratory Medicine, Department of Laboratory Medicine and Pathology, Mayo Clinic, Rochester, MN, USA

⁵Department of Physiology and Biomedical Engineering, Mayo Clinic, Rochester, MN, USA

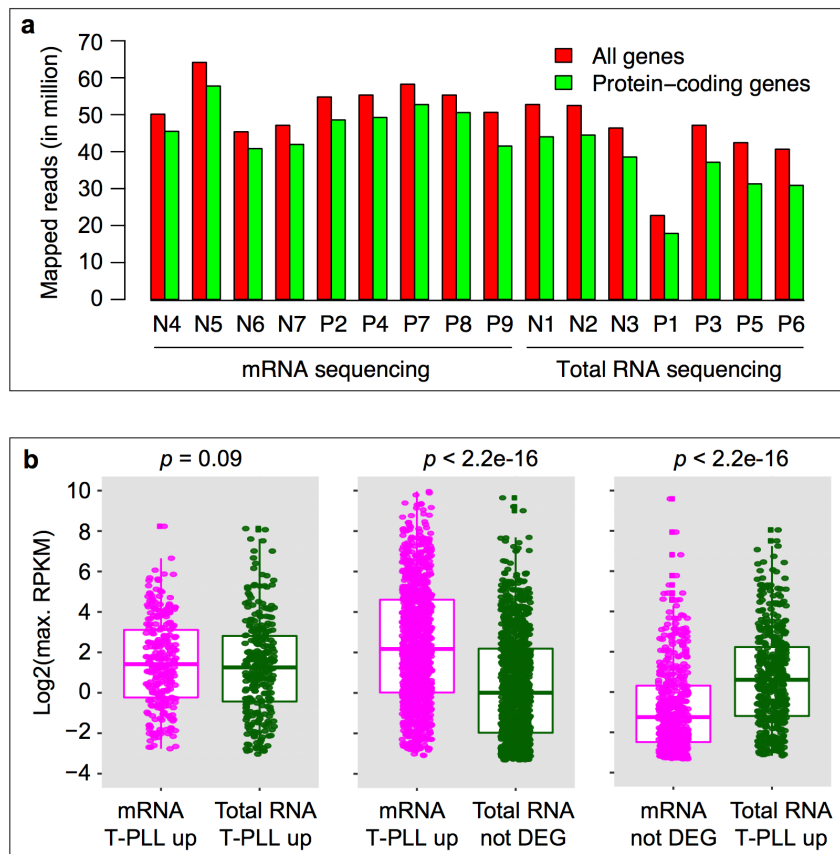
⁶Division of Hematology, Mayo Clinic, Rochester, MN, USA

⁺Current address: Illinois Informatics Institute, University of Illinois at Urbana-Champaign, Urbana, IL, USA

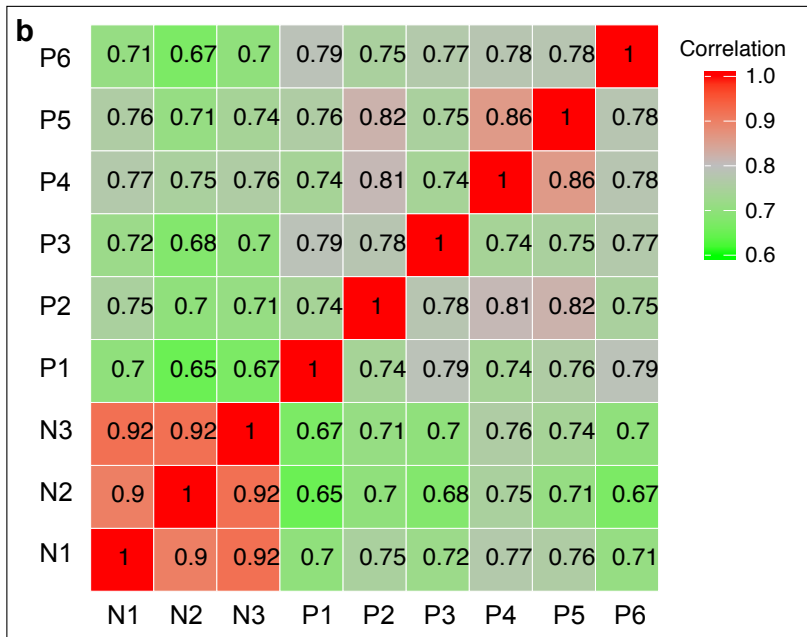
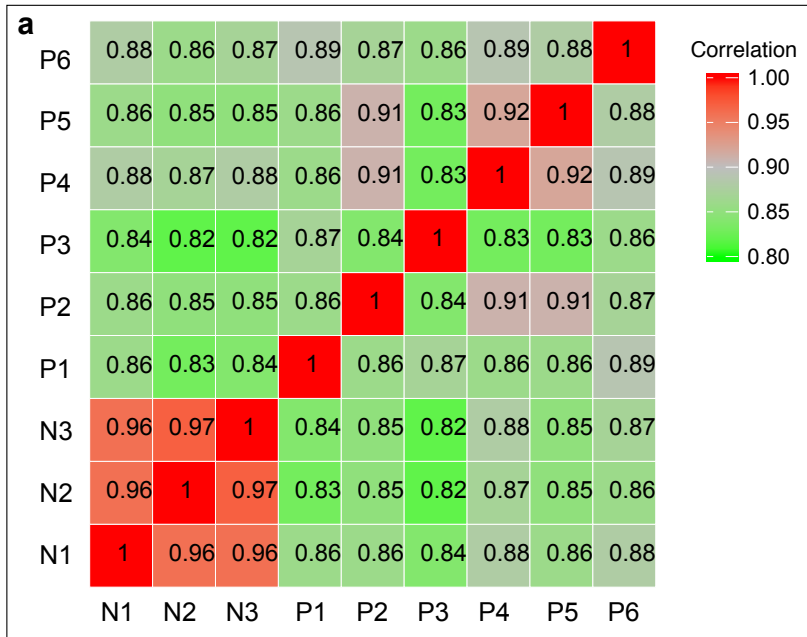
Supplemental Fig. 1 Gene expression changes in T-PLL detected by mRNA sequencing. **(a)** Unsupervised clustering of expression level from top 10 000 most variable genes. N4-N7, normal individuals; P2, P4, and P7-P9, T-PLL patients. Z score was calculated from $\log_2(\text{RPKM}+0.1)$. **(b)** Protein-coding genes differentially expressed between T-PLL and normal. The 2 364 (1466+898) differentially expressed genes were identified using edgeR at the cutoff of 5% FDR and 3-fold change. Y-axis, fold-change at the \log_2 scale; x-axis, sum of the normalized read count per M from the control (normal) and T-PLL group. See Fig. 1 legend for additional information.



Supplemental Fig. 2 Sequencing depth and expression levels of DEGs. **(a)** Total RNA and mRNA sequencing reads mapped to all genes and to protein-coding genes. **(b)** Boxplot showing expression level of protein-coding genes up-regulated in T-PLL revealed by both (left panel), by mRNA sequencing only (middle panel), and by total RNA sequencing only (right panel). The differentially expressed genes (DEGs) were identified using edgeR at the cutoff of FDR \leq 5% and fold change \geq 3. Y-axis represents the gene maximum RPKM value (after log2 transformation with an offset of 0.1) across both T-PLL and normal, calculated separately for mRNA and total RNA sequencing data. P value was calculated using one-sided Mann–Whitney U test (paired=TRUE). Total RNA sequencing was performed for 3 normal (N1-N3) and 4 T-PLL (P1, P3, P5 and P6) and mRNA sequencing for 4 normal (N4-N7) and 5 T-PLL (P2, P4, and P7-P9). See Table 1 for details about sample information.

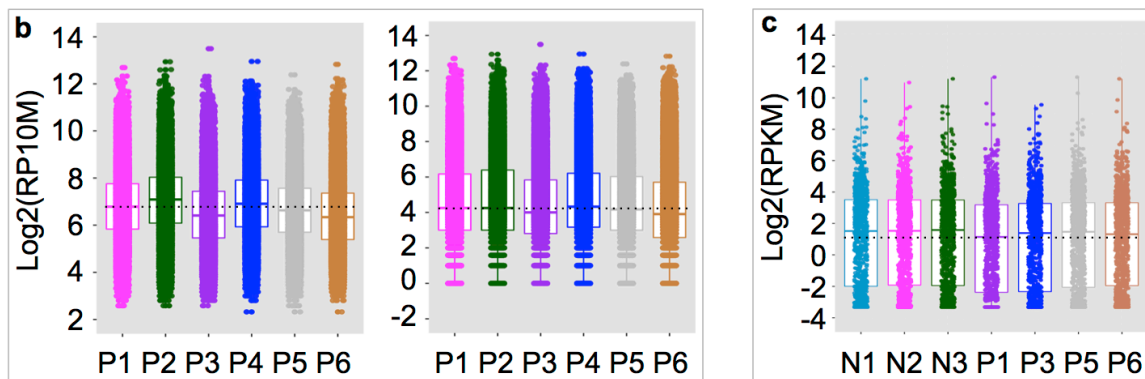


Supplemental Fig. 3 Pairwise Pearson correlation coefficient for H3K4me3 (a) and H3K27ac (b). Only merged peaks from chr1-22 that are present in at least two samples were used. Raw read counts in merged peaks were input-subtracted, normalized to 10M mapped reads, log2 transformed and quantile normalized. N1-N3, normal individuals; P1-P6, T-PLL patients.

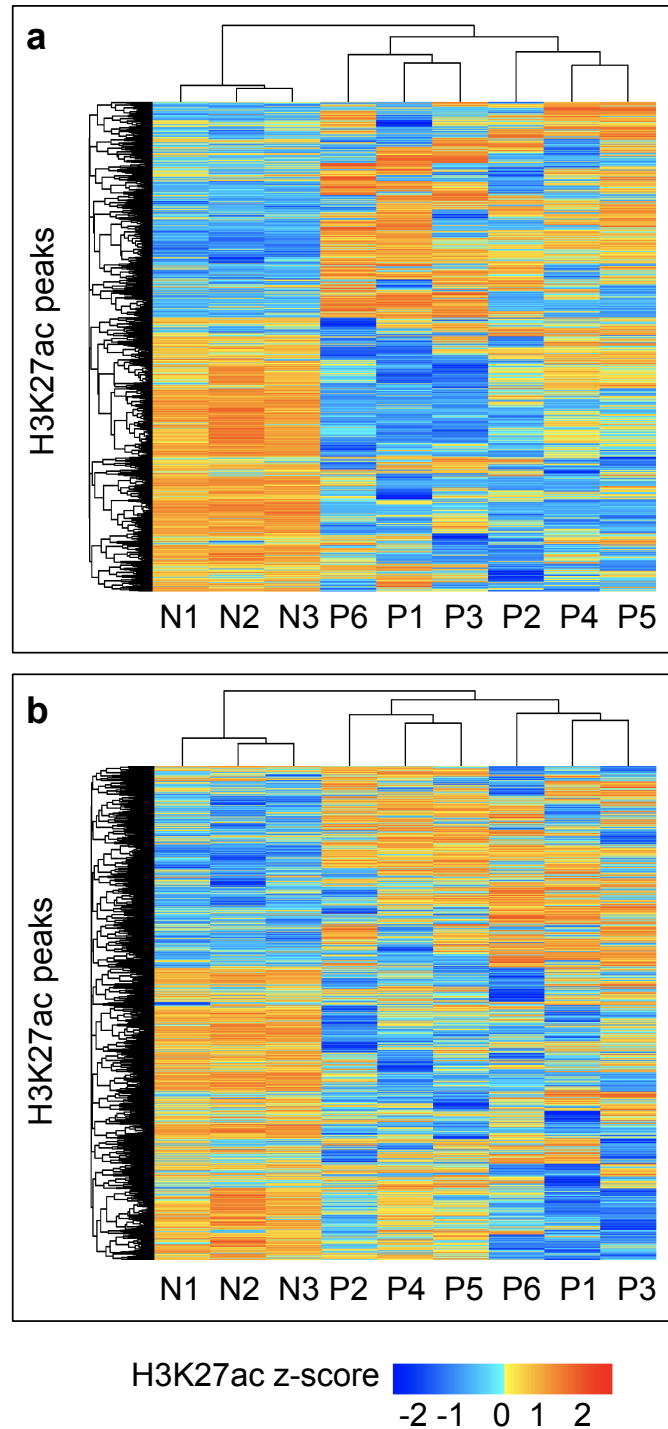


Supplemental Fig. 4 T-PLL H3K27ac summary and tumor suppressor gene expression. **(a)**. Summary of H3K27ac ChIP-seq in 6 T-PLL. ^aHDACi, romidepsin treatment; ^bFC (IP/INPUT fold change), fraction of uniquely mapped reads within peaks in IP / fraction of uniquely mapped reads within peak corresponding regions in INPUT, with duplicate removed; ^cPCC, Pearson correlation coefficient between each T-PLL and the other 5 T-PLL (see Supplemental Fig. 3 for details). **(b)** Signal level of H3K27ac peaks present in all 6 T-PLL (left) and in at least 2 T-PLL (right). RP10M, IP reads per 10M uniquely mapped reads after subtraction of reads from input. Dashed line represents the median $\log_2(\text{RP10M})$ of sample P1. **(c)** Expression level of tumor suppressor genes based on total RNA sequencing. Tumor suppressor genes were from <https://bioinfo.uth.edu/TSGene/>, where only protein-coding genes were used. N1-N3: normal; P1, P3, P5, P6: T-PLL.

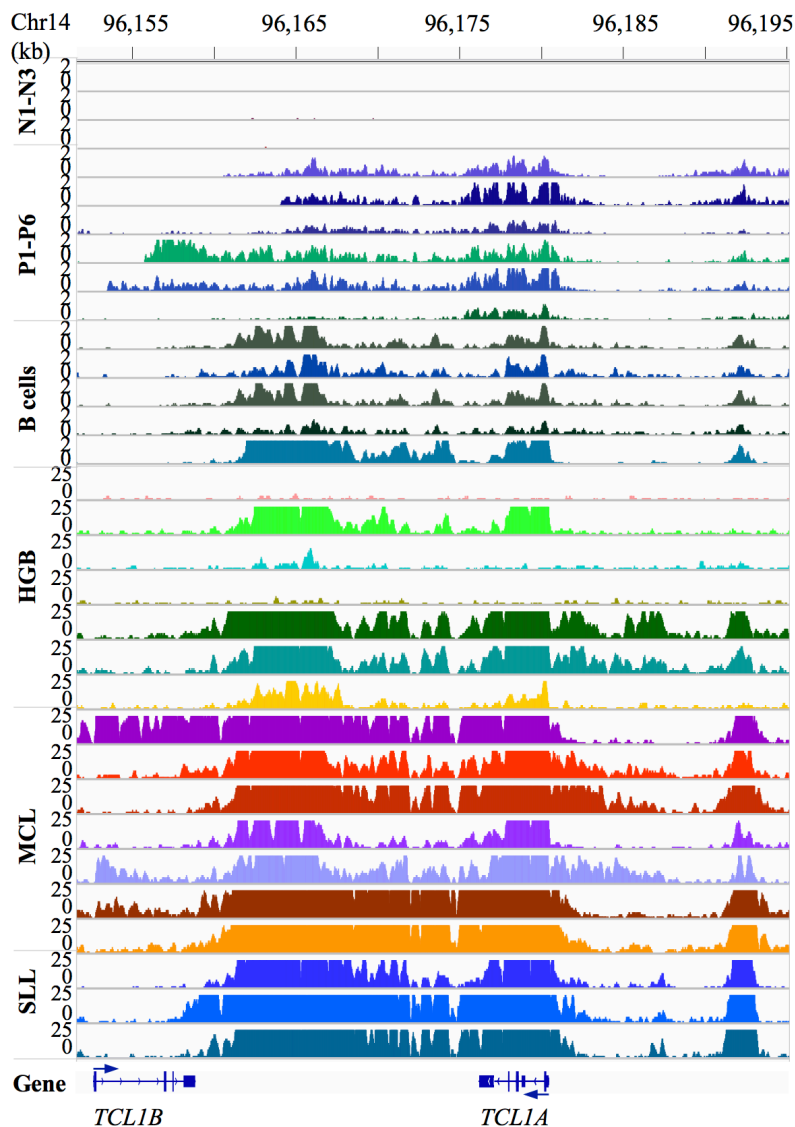
| Sample | HDACi ^a | Usable reads | No. peak | FC ^b | PCC ^c |
|--------|--------------------|--------------|----------|-----------------|------------------|
| P1 | Yes | 27,358,173 | 85,085 | 6.75 | 0.74-0.79 |
| P2 | No | 29,865,798 | 86,364 | 8.14 | 0.74-0.82 |
| P3 | No | 24,393,414 | 79,491 | 6.42 | 0.75-0.79 |
| P4 | No | 21,651,800 | 87,942 | 8.02 | 0.74-0.86 |
| P5 | No | 29,593,013 | 90,794 | 5.6 | 0.75-0.86 |
| P6 | No | 19,815,677 | 69,842 | 5.3 | 0.75-0.79 |



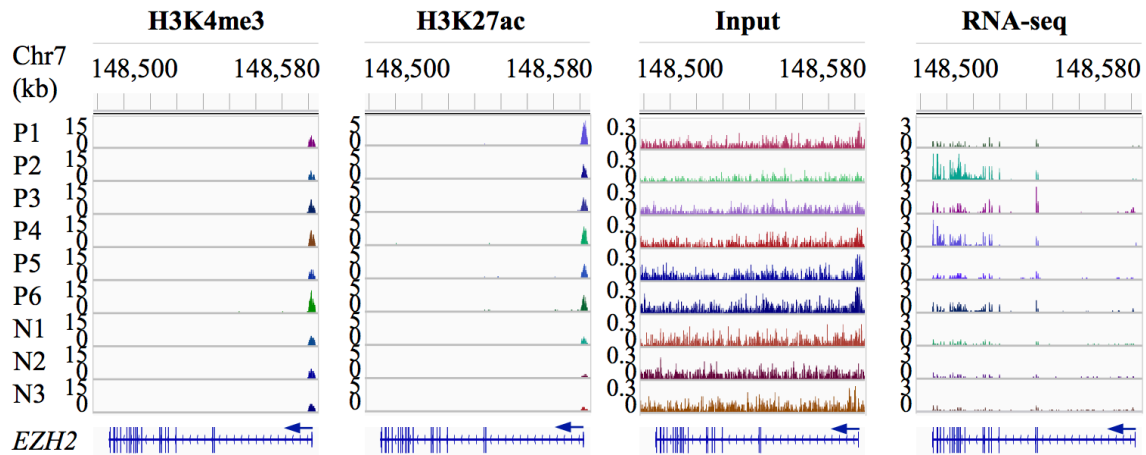
Supplemental Fig. 5 Global alteration of distal H3K27ac peaks in T-PLL. **(a)** Unsupervised clustering of top 10,000 H3K27ac peaks. **(b)** Unsupervised clustering of top 30,000 H3K27ac peaks. See Fig. 2 legend for details.



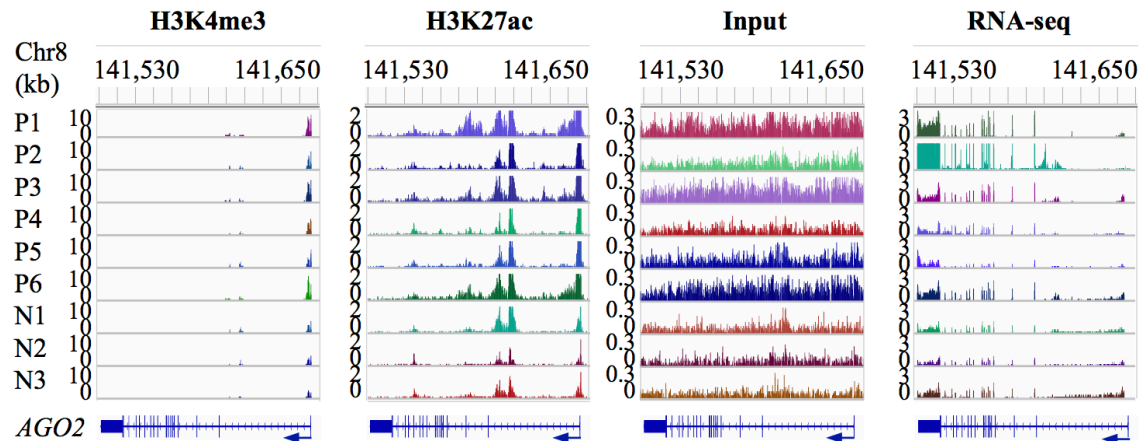
Supplemental Fig. 6 Gained enhancer in *TCL1A* in T-PLL. In the catalog of super-enhancers identified from 86 cell and tissue types, only B cells had the super-enhancer. This super-enhancer was also present in four of the seven high-grade B-cell lymphoma (HGB), all seven mantle cell lymphoma (MCL) and all the three small lymphocytic lymphoma (SLL) patient samples. The raw H3K27ac ChIP-seq reads for four of the five normal B-cell samples were downloaded from GEO under the accession GSM998996, GSM1027287, GSM998997 and GSM2386722. Alignments for the remaining B-cell sample were from Roadmap Epigenomics Project (reference epigenome identifier [EID]: E032).



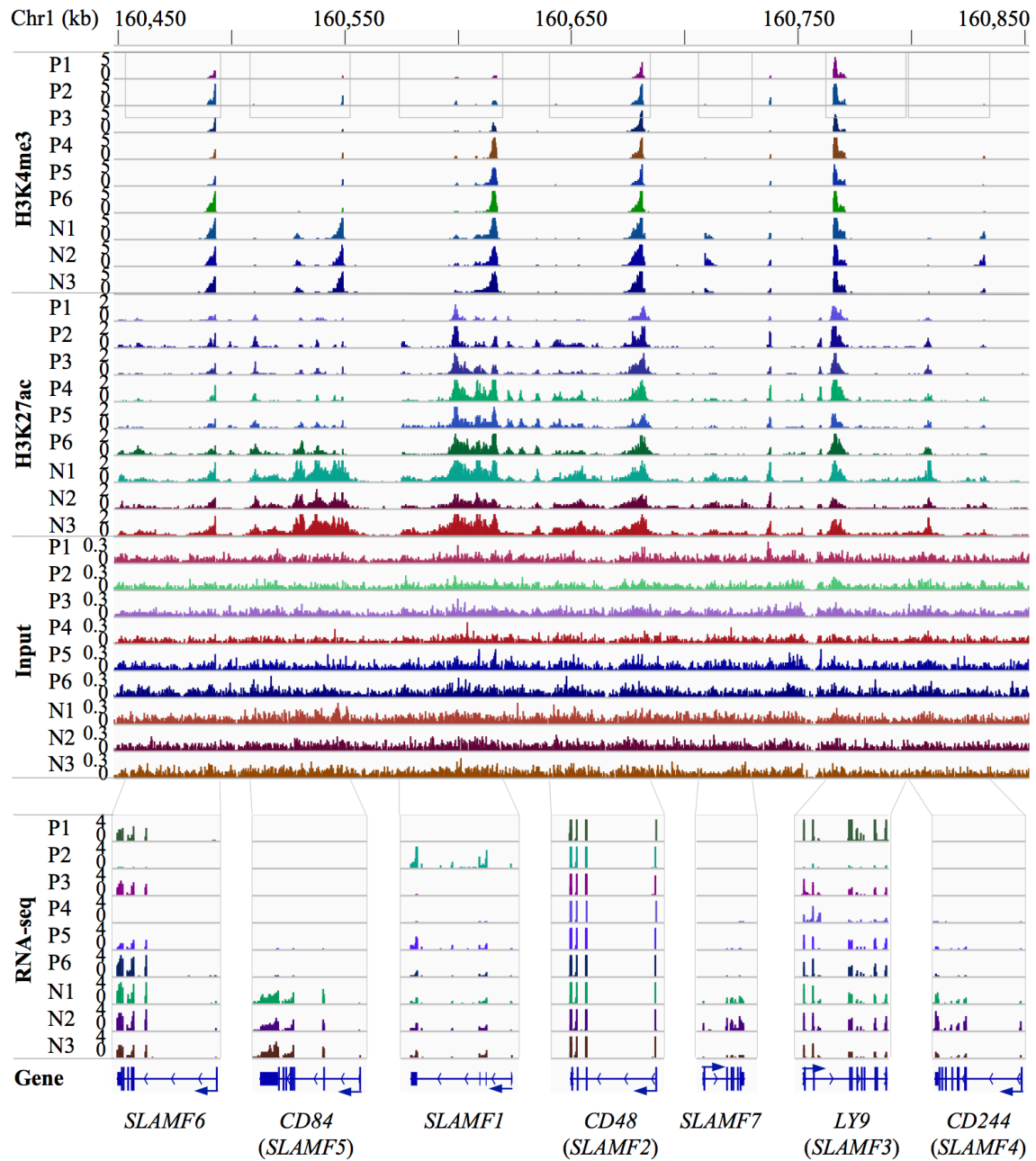
Supplemental Fig. 7 Overall increase of H3K4me3 and H3K27ac in the *EZH2* promoter in T-PLL. *EZH2* was up-regulated in four of the T-PLL cases (P2-P4 and P6). Three of them (P3, P4, and P6) showed increased H3K4me3 and H3K27ac in the promoter. Based on the signal in input, there was a copy-number loss in P2.



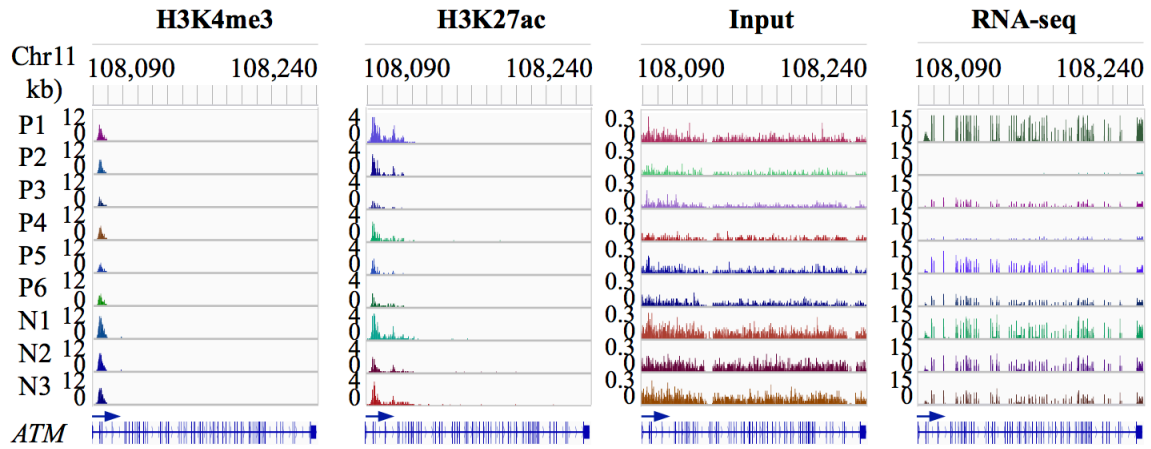
Supplemental Fig. 8 Increased H3K4me3 and H3K27ac in the *AGO2* promoter in T-PLL. All six T-PLL showed increased occupancy of both H3K4me3 and H3K27ac in the *AGO2* promoter. *AGO2* showed elevated expression in two of the T-PLL cases (P1 and P2). Based on input signal, four of the T-PLL (P1, P3, P5 and P6) had copy number gains.



Supplemental Fig. 9 Expression and epigenetic changes in the SLAM family genes. There are seven SLAM family genes in a 378-kb region on chromosome 1. The expression of *CD84*, *SLAMF7* and *CD244* was down-regulated in all T-PLL cases. Accordingly, these genes showed lower levels of H3K4me3 in their promoters. Another two genes, *SLAMF6* and *SLAMF1*, were down-regulated in three T-PLL cases. Of the three, P4 and P5 had lower H3K4me3 in *SLAMF6* promoter and P1 and P3 had lower H3K4me3 in *SLAMF1* promoter.



Supplemental Fig. 10 Reduced H3K4me3 in the *ATM* promoter in T-PLL. All six T-PLL cases showed lower H3K4me3 occupancy in the promoter. *ATM* was down-regulated in four of the T-PLL cases (P2-P4 and P6) that also showed a copy number loss based on input signal.



Supplemental Table 1. Key pathways and GO terms associated with down-regulated genes in T-PLL

| Name | No. gene | Q value | Source |
|--|-----------------|----------------|---------------|
| Immune System | 172 | 4.50E-12 | Reactome |
| Chemokine receptors bind chemokines | 20 | 4.50E-12 | Reactome |
| Peptide ligand-binding receptors | 32 | 4.97E-08 | Reactome |
| Immunoregulatory interactions between a Lymphoid and a non-Lymphoid cell | 26 | 8.70E-08 | Reactome |
| Neutrophil degranulation | 51 | 6.97E-06 | Reactome |
| Signaling by Interleukins | 53 | 1.33E-05 | Reactome |
| Hemostasis | 60 | 2.07E-05 | Reactome |
| Innate Immune System | 98 | 5.19E-05 | Reactome |
| Cytokine Signaling in Immune system | 64 | 1.75E-04 | Reactome |
| Adaptive Immune System | 59 | 4.10E-02 | Reactome |
| Immune response (GO:0006955) | 203 | 1.50E-26 | GO |
| Immune system process (GO:0002376) | 249 | 9.80E-25 | GO |
| Cell activation (GO:0001775) | 147 | 3.57E-22 | GO |
| Regulation of immune system process (GO:0002682) | 150 | 7.90E-19 | GO |
| Defense response (GO:0006952) | 154 | 3.03E-17 | GO |
| Leukocyte activation (GO:0045321) | 121 | 3.28E-15 | GO |
| Positive regulation of immune system process (GO:0002684) | 109 | 2.65E-14 | GO |
| Regulation of immune response (GO:0050776) | 103 | 6.52E-13 | GO |
| Leukocyte mediated immunity (GO:0002443) | 89 | 1.54E-12 | GO |
| Chemokine-mediated signaling pathway (GO:0070098) | 25 | 1.71E-12 | GO |

Gene expression was quantified by mRNA sequencing for four normal (N4-N7) and five T-PLL (P2, P4, and P7-P9).

Supplemental Table 2. Key pathways and GO terms associated with genes up-regulated in T-PLL

| Name | No. gene | Q value | Source |
|--|-----------------|----------------|---------------|
| Erythrocytes take up oxygen and release carbon dioxide | 6 | 2.36E-04 | Reactome |
| O2/CO2 exchange in erythrocytes | 6 | 1.33E-03 | Reactome |
| Extracellular matrix organization | 29 | 1.33E-03 | Reactome |
| MET activates PTK2 signaling | 8 | 5.38E-03 | Reactome |
| Degradation of the extracellular matrix | 16 | 1.95E-02 | Reactome |
| MET promotes cell motility | 8 | 2.89E-02 | Reactome |
| EPHA-mediated growth cone collapse | 7 | 2.89E-02 | Reactome |
| Cell surface interactions at the vascular wall | 15 | 2.89E-02 | Reactome |
| Alpha-defensins | 4 | 3.63E-02 | Reactome |
| G1/S-Specific Transcription | 5 | 4.12E-02 | Reactome |
| Multicellular organism development (GO:0007275) | 269 | 1.12E-07 | GO |
| System development (GO:0048731) | 237 | 8.94E-07 | GO |
| Developmental process (GO:0032502) | 300 | 6.70E-06 | GO |
| Oxygen carrier activity (GO:0005344) | 6 | 9.58E-06 | GO |
| Oxygen binding (GO:0019825) | 9 | 9.22E-05 | GO |
| Circulatory system development (GO:0072359) | 68 | 1.86E-04 | GO |
| Wnt-protein binding (GO:0017147) | 6 | 1.31E-03 | GO |
| Cell differentiation (GO:0030154) | 189 | 1.88E-03 | GO |
| Regulation of cell proliferation (GO:0042127) | 85 | 4.14E-02 | GO |
| Wnt-activated receptor activity (GO:0042813) | 3 | 4.47E-02 | GO |

Gene expression was quantified by total RNA sequencing for three normal (N1-N3) and four T-PLL (P1, P3, P5 and P6).

Supplemental Table 3. Key pathways and GO terms associated with up-regulated genes in T-PLL

| Name | No. gene | Q value | Source |
|---|-----------------|----------------|---------------|
| Axon guidance | 67 | 3.80E-03 | Reactome |
| Signal Transduction | 218 | 8.03E-03 | Reactome |
| Metallothioneins bind metals | 6 | 8.03E-03 | Reactome |
| Neuronal System | 43 | 1.19E-02 | Reactome |
| EPH-ephrin mediated repulsion of cells | 12 | 1.20E-02 | Reactome |
| Extracellular matrix organization | 38 | 1.29E-02 | Reactome |
| EPH-Ephrin signaling | 17 | 1.53E-02 | Reactome |
| Signaling by Interleukins | 57 | 1.94E-02 | Reactome |
| Cytokine Signaling in Immune system | 75 | 2.79E-02 | Reactome |
| Developmental Biology | 101 | 3.04E-02 | Reactome |
| Multicellular organism development (GO:0007275) | 536 | 2.59E-24 | GO |
| Developmental process (GO:0032502) | 601 | 1.71E-23 | GO |
| System development (GO:0048731) | 482 | 6.57E-22 | GO |
| Circulatory system development (GO:0072359) | 130 | 7.51E-10 | GO |
| Cell differentiation (GO:0030154) | 404 | 3.30E-14 | GO |
| Regulation of cell differentiation (GO:0045595) | 198 | 7.81E-11 | GO |
| Wnt-protein binding (GO:0017147) | 10 | 1.63E-03 | GO |
| Wnt-activated receptor activity (GO:0042813) | 8 | 2.49E-03 | GO |
| Transcription regulatory region DNA binding (GO:0044212) | 101 | 1.32E-05 | GO |
| Ephrin receptor activity (GO:0005003) | 9 | 2.07E-04 | GO |

Gene expression was quantified by mRNA sequencing for four normal (N4-N7) and five T-PLL (P2, P4, and P7-P9).

Supplemental Table 4. Copy number alterations in regulatory regions in T-PLL

| Sample | Mark | No. peak* | | No. peak [†] | | Up in T-PLL [§] | | Down in T-PLL [§] | |
|--------|---------|----------------|---------------|-----------------------|---------------|--------------------------|--------------|----------------------------|--------------|
| | | Gain (%) | Loss (%) | Gain (%) | Loss (%) | Gain (%) | Loss (%) | Gain (%) | Loss (%) |
| P1 | H3K27ac | 600 (1.10) | 80 (0.15) | 680 (0.95) | 85 (0.12) | 84 (3.42) | 6 (0.24) | 6 (0.11) | 0 (0.00) |
| P2 | H3K27ac | 1265 (2.31) | 176 (0.32) | 1537 (2.15) | 203 (0.28) | 103 (4.19) | 5 (0.20) | 39 (0.70) | 4 (0.07) |
| P3 | H3K27ac | 1905 (3.48) | 73 (0.13) | 2372 (3.32) | 81 (0.11) | 142 (5.78) | 2 (0.08) | 71 (1.27) | 0 (0.00) |
| P4 | H3K27ac | 425 (0.78) | 42 (0.08) | 484 (0.68) | 46 (0.06) | 27 (1.10) | 1 (0.04) | 9 (0.16) | 0 (0.00) |
| P5 | H3K27ac | 465 (0.85) | 80 (0.15) | 552 (0.77) | 92 (0.13) | 40 (1.63) | 3 (0.12) | 10 (0.18) | 0 (0.00) |
| P6 | H3K27ac | 2850 (5.20) | 69 (0.13) | 3436 (4.80) | 77 (0.11) | 168 (6.84) | 2 (0.08) | 62 (1.11) | 0 (0.00) |
| P1 | H3K4me3 | 366 (1.19) | 41 (0.13) | 507 (1.28) | 53 (0.13) | 21 (1.86) | 8 (0.71) | 27 (0.91) | 2 (0.07) |
| P2 | H3K4me3 | 660 (2.14) | 185 (0.60) | 946 (2.39) | 226 (0.57) | 38 (3.37) | 12 (1.06) | 61 (2.05) | 14 (0.47) |
| P3 | H3K4me3 | 872 (2.82) | 75 (0.24) | 1161 (2.93) | 99 (0.25) | 57 (5.05) | 6 (0.53) | 54 (1.82) | 13 (0.44) |
| P4 | H3K4me3 | 230 (0.74) | 31 (0.10) | 314 (0.79) | 53 (0.13) | 11 (0.98) | 3 (0.27) | 16 (0.54) | 6 (0.20) |
| P5 | H3K4me3 | 203 (0.66) | 124 (0.40) | 293 (0.74) | 146 (0.37) | 8 (0.71) | 3 (0.27) | 21 (0.71) | 4 (0.13) |
| P6 | H3K4me3 | 1489 (4.82) | 69 (0.22) | 2166 (5.47) | 94 (0.24) | 56 (4.96) | 6 (0.53) | 167 (5.62) | 7 (0.24) |

*Number of consensus peaks from chr1-22 that are present in at least two of the six T-PLL with a z-score ≥ 3 (copy number gain) or ≤ -3 (copy number loss). The proportion over the total number of consensus peaks is shown in parentheses.

[†]For consensus peaks from chr1-22 that are present in at least two of the six T-PLL and three normal. These peaks were included in differential analysis between the 3 normal and 6 T-PLL using diffbind package.

[§]Number indicates differential peaks that overlap 100-kb windows with a z-score ≥ 3 or ≤ -3 . The proportion over the total number of differential peaks is shown in parentheses, separately for differential peaks with increased (“Up”) and decreased (“Down”) signal in T-PLL.